



Development and Accuracy Test of a Fused Deposition Modeling (FDM) 3D Printing using H-Bot Mechanism

Budi Hadisujoto *, Robby Wijaya

Department of Mechanical Engineering, Faculty of Engineering and Technology, Sampoerna University, Jakarta, Indonesia

*Corresponding email: ignatius.hadisujoto@sampoernauniversity.ac.id

ABSTRACT

Additive manufacturing process known as the 3D printing process is an advanced manufacturing process including one of the components to support industrial revolution 4.0. The initial development of a 3D printing machine at Sampoerna University is the background of this research. The 3D printing setup of Fused Deposition Modeling (FDM) was built using H-bot moving mechanism by considering the rigidity aspect. The FDM printing method is selected due to its cost and reliability. In this early development, the brackets were custom made using a 3D printer with Polylactic Acid (PLA) material. The result showed that the software worked properly in accordance with the assembled mechanical and electrical parts. The 3D printer could print simple objects such as planes and cubes with small dimensions. However, the printing specimen still lacked accuracy caused by the less rigidity of linear rail brackets, less coplanar belt arrangement, and error in some electronic components.

ARTICLE INFO

Article History:

Received 01 Feb 2021

Revised 02 Mar 2021

Accepted 16 Mar 2021

Available online 17 Mar 2021

Keywords:

3D printing

H-bot

Fused Deposition Modeling

(FDM)

1. INTRODUCTION

The exponentially growing technologies lead to an acceleration in the digital transformation of the traditional manufacturing industry (Wang et al., 2017). The triggered from information and communication technologies (ICT) development has guided industries towards flexible mass

custom production and quantity as the main goal (3dprinting.com, 2019). From that point of view, the smartization of the factory becomes important.

One of the pillars in a smart factory is manufacturing technologies. Additive manufacturing, such as 3D printing, is frequently mentioned as one of the key technologies in Industrial revolution 4.0.

By the integration within the cyber-physical system (CPS), the rapid prototyping method including 3D printing can be accomplished by a direct digital thread. As the result, the production cost could be decreased by 10-30% due to more efficient use of time and resources (3dprinting.com, 2019; Wang et al., 2017; Deloitte, 2014).

Considering the opportunities and challenges, a 3D printing machine needs to be developed and built. It is aligned with the 'Making Indonesia 4.0' by 2018-2030 initiated by the Ministry of Industry Indonesia, which focuses on food and beverage, textile and apparel, automotive, chemical, and electronic (Rojko, 2017). In these industrial sectors, 3D printing technology will become a potentially powerful device.

The objective of this paper is to build and test a 3D printing machine. Fused Deposition Modeling (FDM) was selected as the printing method for this project. The FDM printing method is selected due to its cost and reliability. FDM is a method in which the filament is heated until it reaches a semi-liquid state and then extruded through a nozzle on a platform or previously printed layer (Ngo et al., 2018). This method relies on the thermoplasticity of the material to fuse together during the heating process. The durability of the materials, the stability of mechanical properties, and the suitability of the material for the detailed functional prototype are the main advantages of this method (Materialisme, n.d.).

In this project, the extruder motor is mounted at the frame of the 3D printing separated from the printhead (Bowden Extruder). It produces faster, quieter, and higher quality print due to the less weight of the printhead. The build volume can be larger, in contrast, to direct feed extruders due to a smaller printhead carriage. The size is typically more compact, has less

space in comparison to the direct extruder (Sollmann et al., 2010).

The H-bot mechanism was chosen because of its simplicity in installation and coplanar belt configuration. It consists of two stepper motors, six pulleys, one single belt, three linear rails, three linear guides, and one cart. One motor rotation resulted in a diagonal movement of the print head. Hence, the combination of two motors controls the X and Y axis printing movement. It is expected that the development of this 3D printing can contribute to society, especially the industrial sector.

2. RESEARCH METHODOLOGY

Figure 1 shows the flow chart for building the low-cost FDM 3D printing. The research begins with the selection of printing methods, moving mechanisms, and extruder mechanisms. Followed by the design of the frame and custom brackets, then fabrication. The electronic and electromechanical components also need to be selected and assembled with the frames and brackets. Continued with the software and hardware integration and finished with printing experiments.

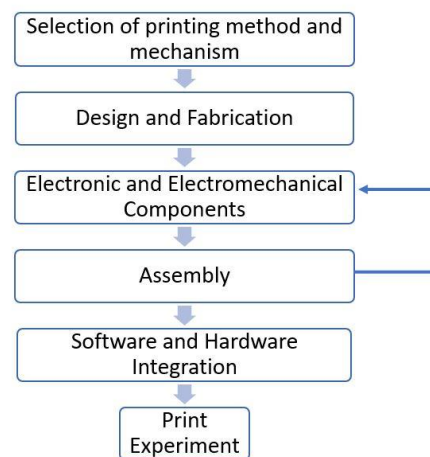


Figure 1. The process of building a low-cost FDM 3D printing.

2.1. Selection of Printing Method and Mechanism

The focus of this project is to build a 3D printing machine that provides a good quality output while minimizing the production cost. Fused deposition modeling (FDM) was chosen as the printing method. Many accessible open-source program scripts and models are available for the FDM project.

Rigidity is typically the main issue of the conventional cartesian (moving platform/bed) and delta (long and thin parallelogram arm) moving mechanism. To overcome this problem, H-bot and Core XY moving mechanisms were considered. The H-bot moving mechanism was chosen because of its advantages, such as simplicity in installation and less backlash risk in comparison to Core XY with many gears and overlap belting arrangement (Shaqour, 2016).

2.2. Design and Fabrication

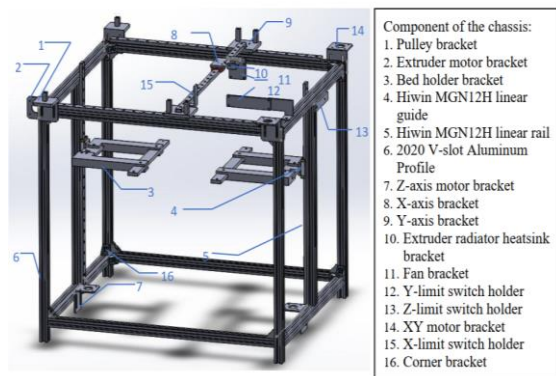


Figure 2. The 3D drawing of the chassis (dimensions are in mm).

Figure 2 shows the main components of the chassis attached to the frame. Almost all of the brackets except the motor brackets and the pulley brackets are made of polylactic acid (PLA) material and manufactured by FDM 3D printing (Anycubic I3). The aim of this chassis is to maximize the build volume of the 3D printing with limit switches and heating elements. The Hiwin MGNH12 linear rails are employed

in the X, Y, and Z axes to enhance the accuracy and precision of the machine.

For the power transmission, the belt arrangement is chosen for the X and Y axes. The lead screw is used for the Z-axis to support the bed holder bracket which holds the weight of the heated bed and specimen.

A 24 cm x 24 cm heated bed is used. The mechanical limit switches are located at X-axis linear rail, Y-limit switch holder bracket, and the frame.

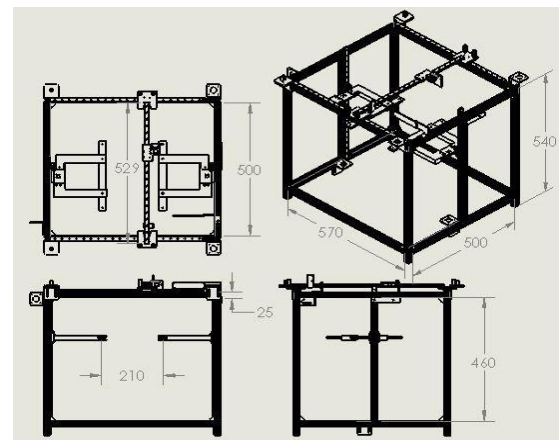


Figure 3. The 2D drawing of the chassis (dimensions are in mm).

Figure 3 shows the 2 dimensions drawing of the front, side, and top views. The maximum build volume of this design is 40 x 40 x 40 cm. The stepper motors and pulley brackets are located at the outside of the frame to maximize the area of the XY plane. The Y-axis linear rails are located at the top of the frame to maximize the z-axis range.

2.3. Electronic and Electromechanical Components

2.3.1. Arduino Mega and Ramps 1.4

Ramps 1.4 as an interface board between Arduino mega and the 3D printer was chosen for its simple connection of electrical to electromechanical components. It has sockets for 5 stepper drivers, screw terminals for 3 heaters, sockets for 3 thermistors, sockets for 6 endstop, and

a slot for SD card. Furthermore, it is considered cheaper in price, has access to open sources, and can readily be integrated into Arduino Mega (Morse, 2019).

2.3.2. Stepper motor NEMA 17

Stepper motor NEMA 17 is a hybrid stepping motor with 200 steps per revolution or 1.8° step angle. The rated voltage is 12 V, with the maximum current is 0.66 Amps. With 3.2 kg-cm allowed holding torque, it can be applied to any type of application. These stepper motors are widely used in 3D printing, CNC machines, precise control machines, laser cutters, and many more (components101.com, 2019).

2.3.3. Stepper Driver A4988

The A4988 micro-stepping stepper motor driver has several features such as adjustable current limiting, over-current and over-temperature protection, and 5 micro-step resolutions ranging from 1 to 1/16 step. It can be operated from 8 to 35 Volts to transfer up to 1 Amp/phase without the need for an additional cooling fin or heat sink. This board is also equipped with 0.1 inches male header pins (Pololu, n.d.).

2.3.4. Endstop Mechanical Limit Switch

The mechanical limit switch is used rather than the optical limit switch due to its lower price, high reliability, and durability, and medium precision. This component was installed to be used as an axis endstop (O'Connell, 2020) and for three axes (X, Y, and Z).

2.3.5. Heated Bed Creality CR 10s V.2

The size of the heated bed is 320 mm by 310 mm. It is suitable for PLA-based materials which can provide approximately up to 70°C. In addition, the surface sheet could be easily removed and installed.

2.3.6. E3D Heater Cartridge

The E3D heater cartridge is used to heat up the filament through the heat block. The diameter is 6 mm with a length of 21 mm, and rated voltage about 12 V to 24 V. It requires 40 watts of power, from the power supply. In this project, it heats up the filament up to 200 °C (E3D, n.d.).

2.3.7. NTC 100 kΩ Thermistor

The NTC 100 kΩ thermistor could read temperature up to 200 °C from the heater. It has 1% precision and can be integrated into the controller. The lower price and its reliability are the main advantages.

2.4. Software to Hardware Integration

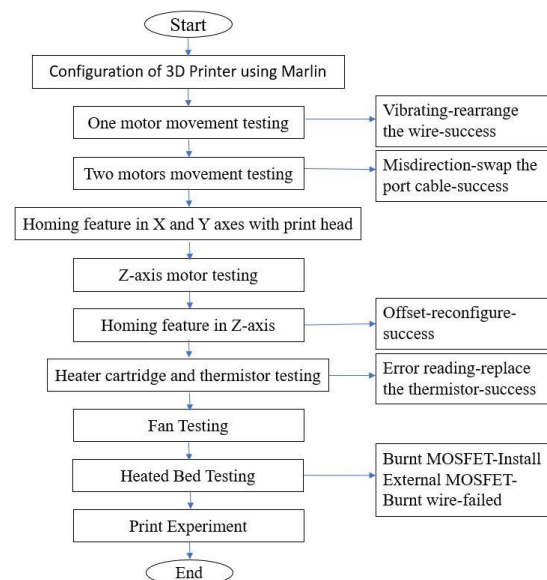


Figure 4. The flow of hardware to software integration.

Figure 4 shows the block diagram of software and hardware integration. There are several issues during the integration process. The marlin firmware as the interface was used to configure the 3D Printer. One motor is tested, followed by two motors, homing feature, Z-axis motor, homing in Z-axis, heating and fan element, then finished print experiment. The vibrating stepper motor, misdirection of the motors, offset of the Z-axis, and error reading of temperature was found. The problems were solved case by case, such as the vibration of motors and misdirec-

tion were solved by rearranging the cable, The Z-offset were solved by reconfiguring the code in the interface software. Error temperature reading caused by the grounding, solved by replacing the thermistor.

2.5. Print Experiment

Three print experiments were held to test the accuracy of the 3D printing. The first is the test print using a square plane shape with 10 cm x 10 cm area and 3 layers of print thickness. The second is the square perimeter, to see the accuracy of the printed object with respect to each axis. The third is the calibration test using the step/unit input modification in the interface.

3. RESULTS AND DISCUSSION

3.1. Y-axis Bracket

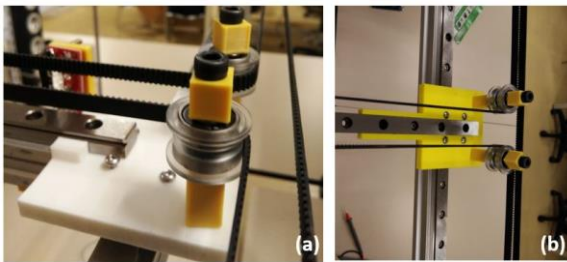


Figure 5. The Y-axis bracket: (a) first design and (b) revised design.

From **Figure 5**, the first design of the bracket holds only one mounting hole of the linear rail. To increase the rigidity, the bracket was revised to be able to hold three mounting holes. The linear rail gains more reaction forces from the fastened-screw and friction from the contact surface of the bracket. The printing result can be observed in **Figure 6**.

The initial design of the Y-axis bracket is shown in **Figure 6 (a)**. The print result demonstrated the inconsistency of the extruded filament. **Figure 6 (b)** shows the result of the revised design of the Y-axis bracket. The square shape becomes more

consistent. This happened due to the incapability of the Y-axis bracket to hold the linear rail which causes a torsional racking, resulting in inaccurate movement of the print head in the XY plane.

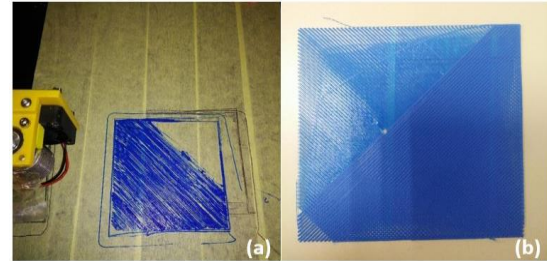


Figure 6. The plane 10 cm x 10 cm: (a) first design Y-axis bracket and (b) revised design Y-axis bracket.

3.2. Square Perimeter Print test

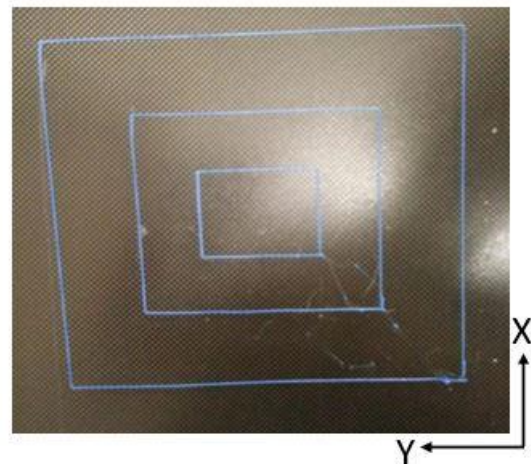


Figure 7. The print result of the square perimeter.

The 3D printing was operated to print three square perimeters with 3 various dimensions, from a small square in the middle to the largest on the outer (**Figure 7**). The results were measured using vernier calipers. To check the accuracy of each motor, the position of the perimeter should be diagonal, following the H-bot mechanism. The error estimation of each perimeter dimension is presented in **Table 1**.

The less coplanar belt arrangement leads to unbalance belt tension which adds more error to the non-rigid Y-axis bracket. The torsional racking emerged

and misdirected printing movement in X-axis. The X-axis linear rail rotated when the torsional racking emerged. This effect shows more significance in a smaller dimension of the square perimeter. The x-axis linear rail is rotated and blocked by belt tension to a certain degree. Hence, the larger dimension experiences a lesser error.

Table 1. Measurement results of the printed square perimeter.

Dimension (mm)	X (mm)	Y (mm)	% error X	% error Y
30x30	25.40	32.20	15.33	7.33
60x60	57.80	64.70	3.66	7.83
100x100	100.40	107.25	0.40	7.25

The least error percentage value is shown in 100 mm x 100 mm square perimeter with 0.4% on X-axis and 7.25% on Y-axis. The error percentage in X-axis is decreased as the dimension is decreased, while the Y-axis is more precise.

3.3. Calibration Test

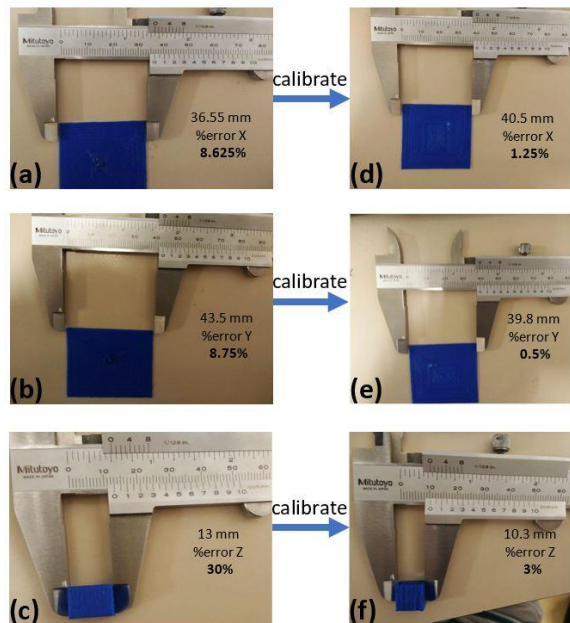


Figure 8. The length measurement of plane 4 cm x 4 cm: (a) X-axis, (b) Y-axis, (d) X-axis after calibration, (e) Y-axis after calibration. The height measurement of 1 cm³ cube: (c) Z-axis, (f) Z-axis after calibration.

Figure 8 shows the calibration test especially the effect of modifying the steps/unit input in the firmware. The step/unit in the program which controls the stepper motor was replaced by a new number with a simple calculation. The ratio between the measured value and true value is multiplied with previous steps/unit value. This ratio will affect the rotation of the motors and convert to linear movement in the XY plane. The result shows improvements in accuracy for all axes.

3.4. H-bot Mechanism Observation

The H-bot mechanism provides a simple mechanism, where a single loop belt connects the extruder cart with the two stepper motors that control the planar x and y axes movements. The configuration of the H-bot seen from the top view is shown in **Figure 9**. Six pulleys are used to direct the belt orientation. The bridge carries the linear rail that provides the x-axis movement of the extruder cart and can move in y-axis direction, where the left and right sides are supported by the y direction two linear rails.

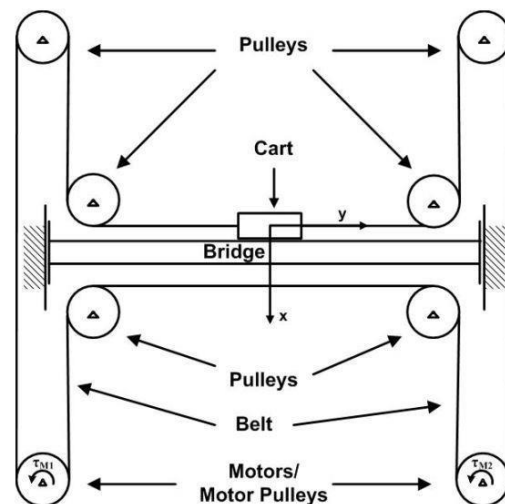


Figure 9. The layout of H-bot moving mechanism (AbdelHamid et al, 2018).

Observing from **Figure 9**, the belt must have an adequate tension to transmit the movements from the two stepper

motors to the extruder cart, while also carrying the load of the bridge and the forces exerted due to the acceleration. Thus, the brackets that support the pulleys for the belt must be strong enough to handle the reaction forces and torques. Deflections of the brackets resulted in dimension printing error, as can be seen in the initial printing attempt of this study.

From this study, it is clear that the material and dimension sizing for the brackets are important. The PLA material has a high elasticity and low strength to be used for a considered big size 3D printer in this research. Furthermore, it is known that the PLA loses its strength over time. Hence thicker brackets were manufactured to overcome the reaction forces and torques. A stronger material with low elasticity, such as steel, is highly recommended for the brackets.

4. CONCLUSION

4.1. Conclusion

The hands-on experience in building a low-cost FDM 3D printing was achieved although the error can be further reduced. Designing the chassis, selecting electronic components, synchronizing the software, electronic, and electromechanical components, as well as testing, were

conducted. The design focuses on maximizing the material and building volume of the 3D printing product. The integration of the software and hardware was successfully achieved. However, the printing result was still not achieved good accuracy nor precision. It can be seen from the error at the perimeter print test. The 3D-printed PLA pulley brackets were the major cause. Furthermore, the less rigid linear rail brackets and non-coplanar belt arrangement worsened the printing result.

4.2. Future Improvement

The performance of 3D printing can be further improved by solving the above-mentioned major causes and some redesign to improve the rigidity of the brackets. The first is to redesign the Y-axis and X-axis brackets that enhance the grip between the linear rails. The second is to fix the belt arrangement and belt tension so that it can achieve a more coplanar H-gantry. The third is to replace the burnt wire with a thicker thickness of wire with good insulation inside. Fourth, is to install a bed leveling sensor such as a proximity sensor or bed leveling touch sensor. Last, is to use a bigger size of the heating bed from 30 cm x 30 cm to 50 cm x 50 cm to maximize the overall build volume of the 3D printing.

REFERENCES

- 3dprinting.com. (2019). *3D Printing flexible filament*. Retrieved from: <https://3dprinting.com/3dprinters/printing-flexible-filament-which-3dprinters-should-you-choose/>
- Abdelhamid, A. Y., Abdeldayem, M., & Mabrouk, M. (2018). Low Cost X-Y Core Positioning System Using Stepper Motor. The 18th International Conference on Applied Mechanics and Mechanical Engineering, AMME-18.
- Components101.com. (2019). *Nema 17 stepper motor*. Retrieved from: <https://components101.com/motors/nema17-stepper-motor/>
- Deloitte. (2014, October 24). *Industry 4. challenge and solutions for the digital transformation and use of exponential technologies*. Retrieved from:

<https://www2.deloitte.com/content/dam/Deloitte/ch/Documents/manufacturing/chemanufacturing-industry-4-0-24102014.pdf/>

E3D. (n.d.). *Standard heater cartridge*. Retrieved from standard heater cartridge: <https://e3d-online.com/products/standard-heater-cartridge/>

Materialise. (n.d.). *Fused deposition modeling*. Retrieved from: <https://www.materialise.com/en/manufacturing/3d-printingtechnology/fuseddeposition-modeling/>

Morse, R. (2019). *Ramps 1.4 review the specs of this controller board*. Retrieved from: <https://all3dp.com/2/ramps-1-4-review-the-specs-of-this-controller-board/>

Ngo, T. D., Kashani, A., Imbalzano, G., Nguyen, K. T. Q., & Hui, D. (2018). Additive manufacturing (3D printing): A review of materials, methods, applications and challenges. *Composites Part B: Engineering*, 143, 172–196. <https://doi.org/https://doi.org/10.1016/j.compositesb.2018.02.012>.

O'Connell, J. (2020). *3D printer endstop switch optical endstop*. Retrieved from: <https://all3dp.com/2/3d-printer-endstop-switch-optical-endstop/>

Pololu. (n.d.). *A4988 stepper motor driver carrier*. Retrieved from: <https://www.pololu.com/product/1182/>

Rojko, A. (2017). Industry 4.0 Concept: Background and overview. *International Journal of Interactive Mobile Technologies (IJIM)*, 11(5), 77-90.

Shaqour, B. (2016). *Developing an additive manufacturing machine*. Staffordshire University. <https://doi.org/10.13140/RG.2.2.10190.77128>.

Sollmann, K. S., Jouaneh, M. K., & Lavender, D. (2010). Dynamic modeling of a two-axis, parallel, H-Frame-Type XY positioning system. *ASME Transactions on Mechatronics*, 15(2), 280–290.

Wang, X., Jiang, M., Zhou, Z., Gou, J., & Hui, D. (2017). 3D printing of polymer matrix composites: A review and prospective. *Composites Part B: Engineering*, 110, 442–458. <https://doi.org/https://doi.org/10.1016/j.compositesb.2016.11.034>.